Nanoscale

PAPER

View Article Online
View Journal

Cite this: DOI: 10.1039/c4nr04387a

Cyclic chlorine trap-doping for transparent, conductive, thermally stable and damage-free graphene†

Viet Phuong Pham,‡[a] Kyong Nam Kim,‡[b] Min Hwan Jeon,[a] Ki Seok Kim[b] and Geun Young Yeom*[a,b]

Received 1st August 2014,
Accepted 29th October 2014

DOI: 10.1039/c4nr04387a

www.rsc.org/nanoscale

We propose a novel doping method of graphene using the cyclic trap-doping method with low energy chlorine adsorption. Low energy chlorine adsorption for graphene chlorination avoided defect (D-band) formation during the doping by maintaining the π-bonding of the graphene, which affects conductivity. In addition, by trapping chlorine dopants between the graphene layers, the sheet resistance could be decreased by ~88% under optimized conditions. Among the reported doping methods, including chemical, plasma, and photochemical methods, the proposed doping method is believed to be the most promising for producing graphene with extremely high transmittance, low sheet resistance, high thermal stability, and high flexibility for use in various flexible electronic devices. The results of Raman spectroscopy and sheet resistance showed that this method is also non-destructive and controllable. The sheet resistance of the doped tri-layer graphene was 70 Ω per sq. at transmittance of 94%, and which was maintained for more than 100 h in a vacuum at 230 °C. Moreover, the defect intensity of graphene was not increased during the cyclic trap-doping.

Introduction

Graphene has attracted much attention owing to its remarkable mechanical and electrical properties and is being actively developed to realize its full potential.[1–7] Some of its important properties are suitable for making transparent conductive films: high conductivity, high transparency, and excellent flexibility; because of these superior properties, graphene has been studied as a possible replacement for indium tin oxide (ITO).[9–11,13–15] Its serious disadvantages, however, have been the relatively high sheet resistance (~a few hundred Ω per sq.) compared to that of ITO (a hundred Ω per sq.) under similar optical transmittance conditions and the difficulty in scaling it to large size. With regard to the latter, many approaches and advances have been reported for the synthesis of graphene by large area chemical vapor deposition (CVD).[8–11,13–16] The former, *i.e.*, the relatively high sheet resistance, has been a bottleneck for its application to transparent conductive films. The sheet resistance of ideal graphene is much lower than that of the CVD graphene reported.[9] The higher sheet resistance of CVD graphene originates from and is strongly dependent on defects in the crystal, wrinkles, and the grain and domain sizes of the actually grown graphene layers. For these reasons, researchers have tried to improve the sheet resistance by various doping methods, including chemical,[11,12,17] plasma,[18–20] and photochemical methods.[20] However, many problems still remain to be solved, such as the much higher sheet resistance than that of ITO under similar optical transmittance conditions, the transmittance degradation during chemical doping, the thermal instability and serious damage during plasma doping, *etc.*

For example, in the case of wet chemical doping, Gunes *et al.* showed the possibility of achieving low sheet resistance by chemical doping, and obtained a sheet resistance of 54 Ω per sq. using four graphene layers.[11] However, their doping process showed the relatively poor transmittance of 85% because of the agglomeration of Au ions by the $AuCl_3$ chemical they used. In addition to this process, various other chemical doping processes have also been investigated to improve the sheet resistance and transmittance.[17,20–24] However, these methods did not satisfy both low sheet resistance and high transmittance at the same time. As another technique, Li *et al.* tried to reduce the sheet resistance using the photochemical doping process.[25] The sheet resistance they obtained, however, was significantly increased by about 3 orders of magnitude.

[a]SKKU Advanced Institute of Nano Technology (SAINT), Sungkyunkwan University (SKKU), Suwon, Gyeonggi-do 440-746, Republic of Korea. E-mail: gyyeom@skku.edu
[b]School of Advanced Materials Science and Engineering, Sungkyunkwan University (SKKU), Suwon, Gyeonggi-do 440-746, Republic of Korea

† Electronic supplementary information (ESI) available. See DOI: 10.1039/c4nr04387a

‡ These authors contributed equally to this work.

This result meant that the photochemical method interrupted the conducting system of graphene, and introduced damage-inducing scattering centers.

In this study, we propose an innovative method for doping graphene to realize a graphene film with low sheet resistance, high transparency and high thermal stability while maintaining the nature of graphene. To realize a graphene film having these properties, we used the cyclic trap-doping method with low energy chlorine adsorption. The graphene film synthesized by chemical vapor deposition (CVD) was transferred to PET and quartz films for low energy chlorine doping. Our results demonstrated that the graphene network was not destroyed by low energy adsorption. The proposed method produced graphene films with a high transmittance of 94% at 550 nm and a sheet resistance of 70 Ω per sq. with excellent thermal stability after two cyclic chlorine trap-doping processes.

Results and discussion

Fig. 1 shows a schematic flow chart of the cyclic trap-doping strategy for multilayer graphene. Pristine CVD-grown monolayer graphene was transferred onto various substrates and was chlorinated by chlorine adsorption. In this chlorine doping process, low energy radicals extracted from the chlorine plasma confined by a double-mesh grid system were used to prevent damage to the graphene (see Fig. S1, ESI†). When the Cl radical is adsorbed on the graphene surface, due to the strong electronegativity of the Cl atom, an electron is transferred from the graphene surface to the attached Cl atom, and an ionic bonding between the graphene surface and the Cl atom is formed without breaking the graphene structure. Generally, during the plasma doping for the previous research studies, graphene was damaged by breaking the C–C bonding in the graphene (the C–C bond strength in graphene is very delicate at 4.9 eV) due to the ion bombardment during the exposure to the plasma. In our Cl plasma, we used a double mesh-grid shown in Fig. S1† to remove ion energy bombardment during the Cl plasma operation and to disallow breakage of the graphene network by the ions. Generally, chlorine dopants adsorbed on a graphene film surface can be easily removed during the handling of the graphene under various environmental conditions such as heating, moisture, oxygen, *etc.* For this reason, in addition to low energy chlorine doping,

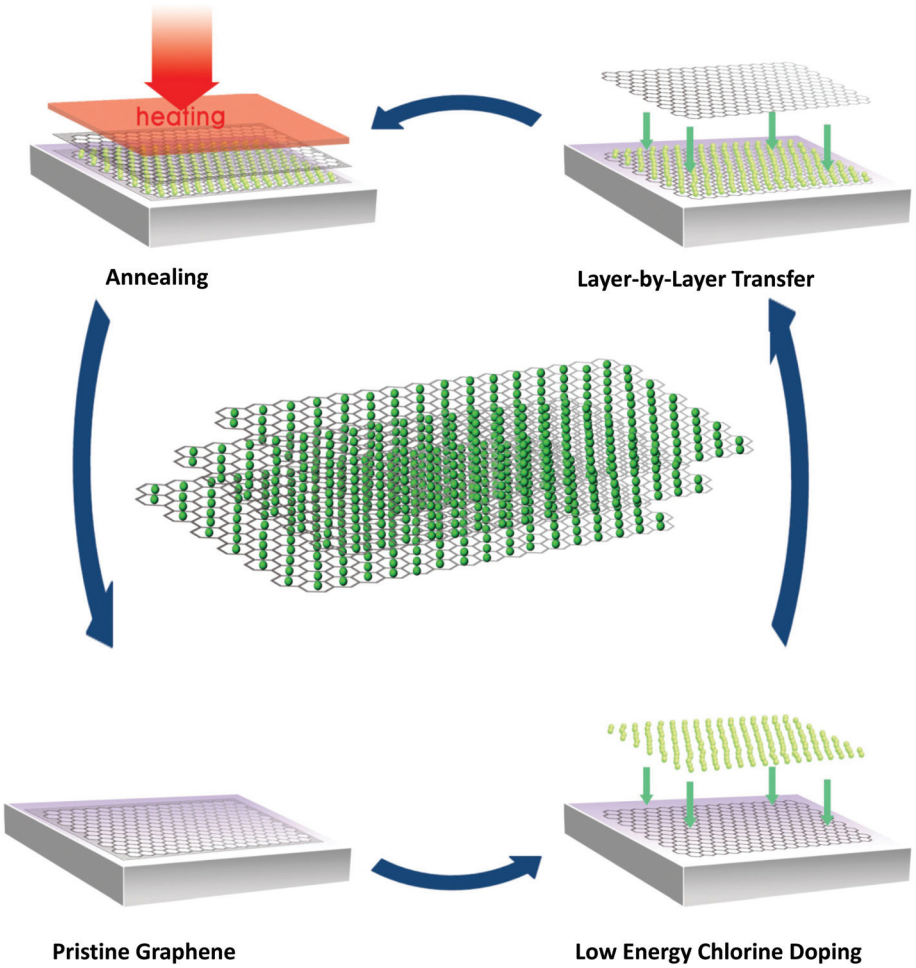

Fig. 1 A schematic flow chart for the multi-layer cyclic trap-doping strategy: one cycle of trap-doping includes low energy chlorine doping, graphene transfer, and annealing processes.

the method of confining chlorine dopants between graphene films by transfer of a second graphene layer on the doped graphene layer has been used for the bi-layer doped graphene. For the tri-layer doped graphene, after the transfer of the second layer, chlorine doping was repeated on the second graphene layer, followed by the transfer of the third graphene layer on top of the second graphene layer, *etc.* Therefore, through the cyclic low energy chlorine doping and transfer strategy, multi-layer doped graphene can be prepared. During cyclic chlorine radical doping, just after the transfer of each graphene layer, the graphene was annealed in a vacuum furnace at 250 °C for the SiO_2 and quartz substrates, and at 230 °C for the PET film for 30 min.[26]

To understand the effect of chlorine doping by low energy chlorine adsorption using chlorine plasma, a Raman analysis was carried out. The doping effect can be observed through the changes in the peak positions of the G and 2D bands. Fig. 2(a) shows the Raman spectra data for a mono-layer graphene sample before and after the chlorine doping process using low energy chlorine radicals for 25 s and after heating in a vacuum furnace at 230 °C for 6.5 h. Fig. 2(b) and (c) are the zoom-in spectra of the Raman G and 2D peaks shown in Fig. 2(a), respectively. The chlorine plasma was generated at 20 W of rf power with 60 sccm 10 mTorr Cl_2. From previous research studies, it is found that, in the case of conventional plasma doping techniques, serious defects are generally formed in the graphene network because the energetic ions and electrons in the plasma bombard the graphene surface and destroy the sp^2 bonded carbon network of graphene. As the characteristic disorder-induced D band emerges, the 2D band intensity is decreased significantly and the G band is also broadened[18,27,28] (see Fig. S2, ESI†). The damage and severe degradation of the graphene film by these methods significantly limit the application of the graphene film to various electronic devices. As shown in Fig. 2(a), after chlorine radical doping with low energy chlorine radicals, the D peak intensity of graphene did not increase, indicating that there was no noticeable degradation of graphene after the doping even though the I_D/I_G ratio was slightly increased from 0.07 to 0.09. However, as shown in Fig. 2(b) and (c), G and 2D peak positions were blue-shifted by 5 cm^{-1} and 7 cm^{-1}, respectively. We heated the doped graphene in a vacuum furnace at 230–250 °C for 100 h and checked its reversibility through the Raman shift. If this doping method does not affect the graphene network, then

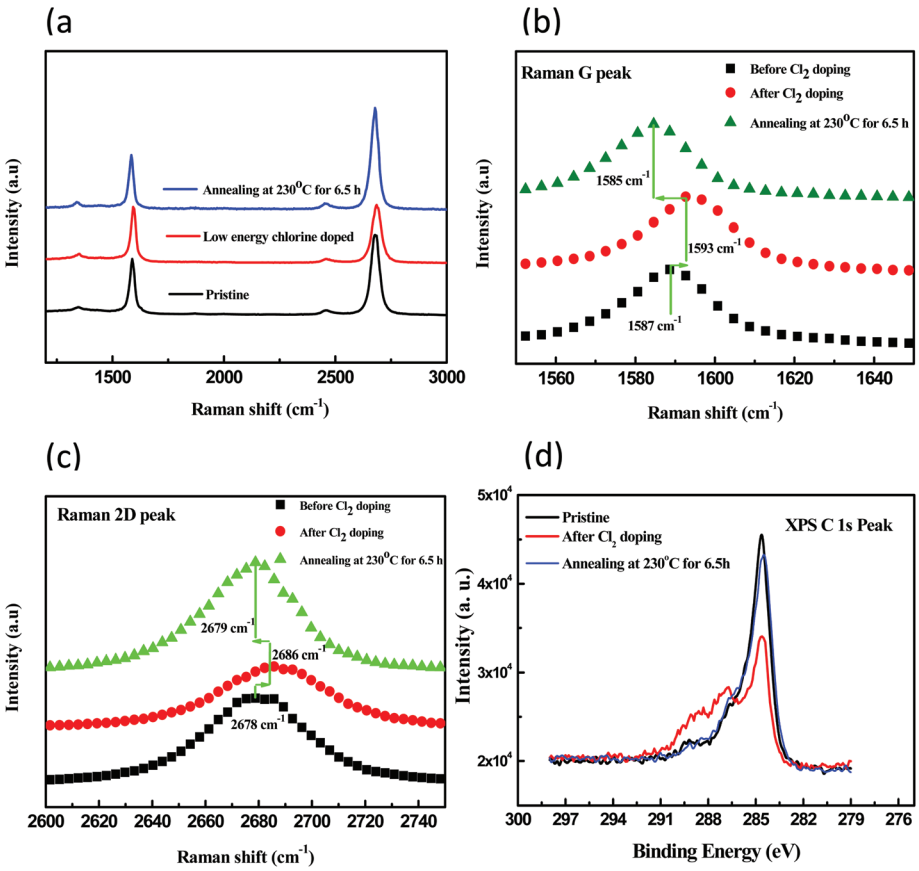

Fig. 2 (a) Raman spectra data for a monolayer graphene sample before and after the chlorine doping process using the low energy chlorine radicals, and after heating at 230–250 °C for 6.5 h. The chlorine plasma was generated at 20 W of rf power with 60 sccm 10 mTorr Cl_2. (b) Zoom-in spectrum of the Raman G peak before/after chlorine doping and after heating at 230–250 °C for 6.5 h. (c) Zoom-in spectrum of the Raman 2D peak before/after chlorine doping and after heating at 230–250 °C for 6.5 h. (d) XPS C 1s spectra of the pristine monolayer graphene and chlorine doped mono-layer graphene after annealing at 230–250 °C for 6.5 h.

after the removal of dopants through heating, the doped graphene should change back to pristine graphene. As shown in the figures, after heating in a vacuum furnace at 230–250 °C for 100 h, the Raman shifts of G and 2D peaks by chlorine doping returned back to their original positions, indicating that there was no damage to the graphene during doping by the low energy chlorine doping method. Fig. 2(d) shows the X-ray photoelectron spectroscopy (XPS) C 1s narrow scan spectra of the pristine mono-layer graphene, chlorine doped mono-layer graphene and after heating in a vacuum furnace at 230–250 °C for 100 h. In the chlorine doped mono-layer graphene sample, a C–Cl bonding peak at 286.8 eV due to chlorine doping on the graphene surface and a C–O bonding peak at 289 eV attributed to the presence of carbon oxide contaminations were observed. However, after heating, the C–Cl bonding peak was significantly removed and recovered close to that of the pristine mono-layer graphene. From these consistent results, the method of chlorine doping through low energy chlorine adsorption is believed to be an effective method for damage-free graphene doping. Therefore, we proceeded to investigate the chlorine trapping between the graphene layers overlapping with each other in order to eliminate the above drawbacks as illustrated in Fig. 3.

In fact, for damage-free graphene doping, the plasma conditions need to be optimized such that high energy chlorine ions do not bombard the graphene surface. Using low energy chlorine radicals, we carried out doping experiments with mono-layer graphene and observed the variation in sheet resistance according to the beam conditions (see Fig. S3, ESI†). In low energy radical doping using chlorine plasma with the double-mesh grid system, the number of chlorine radicals passing through the mesh grid depends on the operation conditions such as rf power, plasma exposure time, *etc.* The increase of rf power increases not only the chlorine radical density in the plasma but also the possibility of damaging the graphene by increased high energy ion bombardment. The increase of the plasma exposure time increases the chlorine radical dose to the graphene. From these results, the chlorine plasma with the double-mesh grid could be used to control and optimize the degree of doping without damaging the graphene film. Under optimized conditions, the sheet resistance of the graphene was decreased by more than 50% compared to that of the pristine monolayer graphene film.

Generally, the effect of chlorine radical doping through pure chemisorption accompanied by the breaking of the sp^2 C–C bonding followed by the formation of C–Cl bonding can be maintained for a longer time than that of chlorine radical doping through the physisorption of Cl on C–C bonding. However, by chlorine radical doping through pure chemisorption, the graphene structure is damaged and sheet resistance is increased by 3 orders of magnitude.[20] This highly resistive graphene film cannot be applied to various electronic applications including transparent conductive films. On the other hand, in the case of chlorine radical doping through physisorption, chlorine atoms are weakly bonded to the graphene surface; therefore, it is difficult to maintain the doping effect

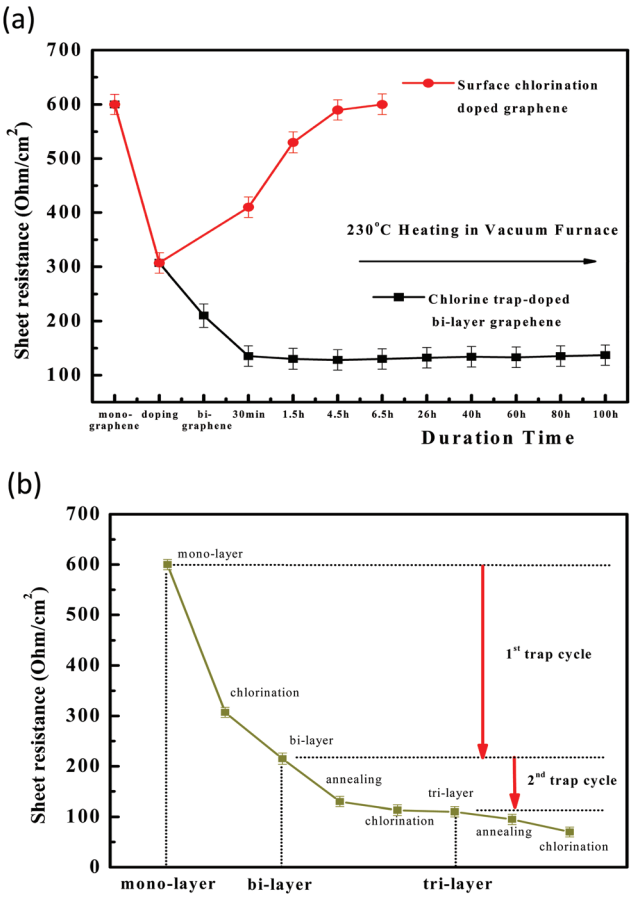

Fig. 3 (a) The changes of sheet resistance with heating time after surface chlorine radical doping of monolayer graphene and after chlorine trap-doping in a bilayer graphene. The chlorine radical doping conditions were the same as those described in Fig. 2 and the heating of graphene was conducted in a vacuum furnace at 230 °C for 30 min to 100 h. (b) The change of sheet resistance through the cyclic trap-doping which includes 1st cycle of trap-doping (chlorine doping, transfer of the 2nd graphene layer, annealing) and 2nd cycle of trap-doping (2nd cycle of chlorine doping, transfer of the 3rd graphene layer, annealing). The annealing was also conducted at 230 °C in a vacuum furnace.

for a long time. For this reason, we trapped the chlorine radical dopants between the graphene layers using the trap-doping technique and studied the effect of trap-doping on the thermal stability and sheet resistance of the graphene structure. Fig. 3(a) shows the changes of sheet resistance with heating time after the surface chlorine radical doping of mono-layer graphene and that after the chlorine trap-doping in a bi-layer graphene structure, which includes chlorine doping and trapping between two graphene layers. The chlorine radical doping conditions were the same as those described in Fig. 2 and the graphene was heated in a vacuum furnace at 230 °C for 30 min to 6.5 h to investigate the thermal stability of the doped graphene. As shown in the figure, for the mono-layer graphene, after the surface chlorine radical doping, the sheet resistance became 50% of that of pristine graphene. However, after the doped monolayer graphene was heated in a vacuum furnace at 230 °C for 100 h, the sheet

resistance returned to the level of the pristine graphene because the volatile chlorine dopants were removed from the surface of the graphene film during the heating. However, in the case of the trap-doped bi-layer graphene structure, the sheet resistance further decreased after heating for 30 min and did not change significantly with increasing heating time up to 6.5 h. Therefore, the trap-doped bi-layer graphene structure remained stable after the doping.

In addition, as shown in Fig. 3(b), through the cyclic trap-doping, which includes the 1st cycle of trap-doping (chlorine doping, transfer of the 2nd graphene layer, annealing), 2nd cycle of trap-doping (2nd cycle of chlorine doping, transfer of the 3rd graphene layer, annealing), *etc.*, the sheet resistance of the tri-layer graphene structure decreased significantly to about 70 Ω per sq. The annealing was also conducted at 230 °C for 30 min in a vacuum furnace. The significantly low sheet resistance of a tri-layer graphene is related to the doping effect, which incidentally does not form any scattering centers in the graphene layers because chlorine doping through physisorption does not interrupt the conjugated system of the graphene composed of conducting π-bonds (see Fig. S4, ESI†). In addition to the low energy chlorine radical doping itself, the optimization of the annealing condition after the trap-doping will play an important role in the decrease of the sheet resistance because in our results, the sheet resistance was further decreased by about 40% and 14% after the annealing of 1st and 2nd trap-doping, respectively. These decreases are believed to arise from the annealing of the defects in the graphene layers with chlorine radicals trapped between the graphene layers. Finally, the result shows that the trap doping method is very stable and can be used as a damage-free graphene doping method in combination with the low energy chlorine radical doping used for the mono-layer graphene.

Using transmission electron microscopy (TEM), the location of chlorine atoms in the chlorine trap-doped graphene was investigated. Fig. 4(a) and (b) show low-magnification color-scaled DF (dark field)-TEM images of a bi-layer graphene without (pristine) and with the chlorine trap doping process using the low energy radicals, respectively. Wide brown colored areas in Fig. 4(b) are believed to be related to the locations of chlorine atoms between the graphene layers caused by the trap doping of chlorine. A thin network of brown color is also shown in Fig. 4(a) and, even though it is not clear this time, it is believed to be from the slight doping of Cl on the graphene from a $FeCl_3$ etchant used during the graphene transfer process (see the Experimental section). The existence of Cl atoms in the brown colored area was confirmed through micro-EDS (energy dispersive X-ray spectroscopy) in TEM (see Fig. S5, ESI†).

Fig. 5 shows the optical transmittance of the mono-layer and tri-layer chlorine doped graphene on PET substrates. The

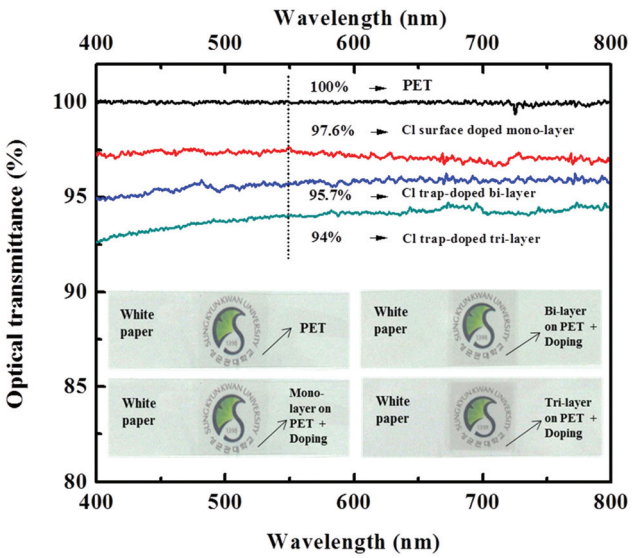

Fig. 5 The optical transmittance measured using UV-Vis-NIR spectroscopy for the PET substrate itself and the doped graphene on PET substrates with mono-, bi-, and tri-layer graphenes. White paper is the area without any PET film.

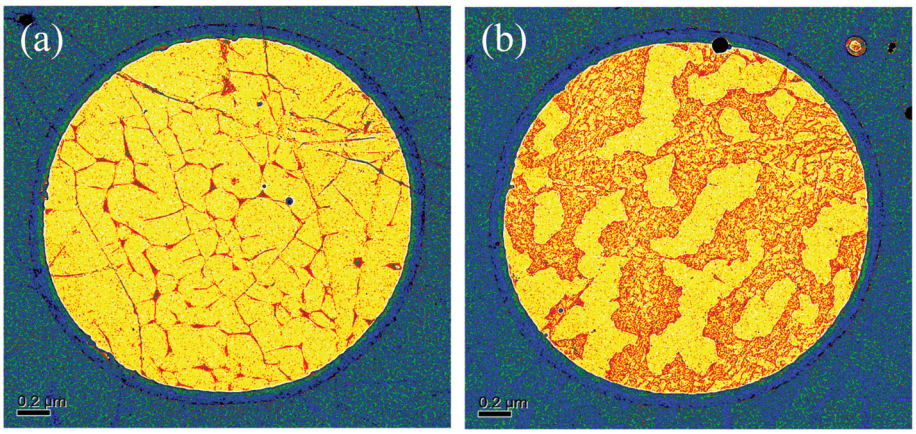

Fig. 4 Low-magnification DF-TEM images of a bi-layer graphene with/without trap doping. (a) DF-TEM image of pristine bi-layer graphene and (b) DF-TEM image after the chlorine trap-doping in a bilayer graphene. The chlorine radical doping conditions were the same as those described in Fig. 2. The wide brown color areas in (b) are related to the chlorine atoms between the graphene layers.

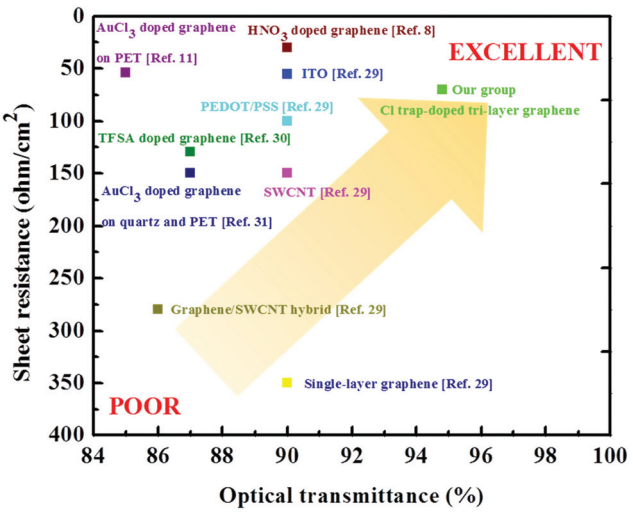

Fig. 6 Comparative analysis of various transparent conductive films reported in recent research studies in the aspects of transmittance and sheet resistance.

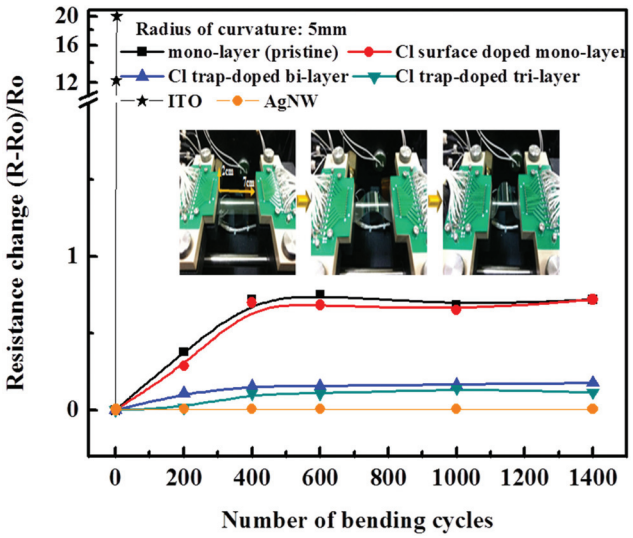

Fig. 7 Sheet resistance change during the bending of the graphene on PET substrates. The pristine monolayer graphene layer and the doped graphene layers (mono-, bi-, tri-layer) were prepared on 100 μm thick PET substrates and were bent with a curvature radius of 5.0 mm at a frequency of 1 Hz.

pristine mono-layer graphene showed a high transmittance of ~97.6% (±0.3%) at 550 nm. After the chlorine radical doping, although the sheet resistance was decreased by 50%, the transmittance remained the same as that of the pristine graphene. As the chlorine doping was repeated to tri-layer by cyclic trap-doping, the transmittance changed to ~94%. This indicates that chlorine trap-doping did not deteriorate the optical transmittance, but only reduced the optical absorption when the graphene film layer is increased to tri-layer.

Fig. 6 shows that a comparative analysis of the transmittance and sheet resistances of various transparent conductive films.[8,11,29–31] As shown in the figure, some films show the highest transmittance with high sheet resistance while other films show the lowest sheet resistance with a low optical transmittance. Among the transparent conductive films investigated, the tri-layer graphene doped by the cyclic trap-doping strategy showed the excellent properties of both low sheet resistance and high transparency. Moreover, as mentioned above, this cyclic trap-doping strategy can be the most powerful doping technique for realizing doping stability according to the environment.

ITO has been an excellent material for transparent electrode applications. However, with the industry of transparent electrode applications moving toward the development of flexible electronics, ITO has shown many limitations in flexibility, such as bending, stretching, *etc.* Fig. 7 shows the change of sheet resistance during the bending of the graphene on PET substrates. A pristine mono-layer graphene layer and doped graphene layers (mono-, bi-, and tri-layer) were prepared on 100 μm thick PET substrates and were bent 1400 times with a curvature radius of 5.0 mm at a frequency of 1 Hz. The reduced resistance $(R - R_0)/R_0$ plotted in the figure indicates the ratio of the change of the sheet resistance to the initial resistance. The bending results of ITO and AgNW are provided.[9] In the bending test of the AgNWs conductive film, the sheet resistance was not significantly changed as the number of bending cycles was increased while the ITO film showed an abrupt increase of sheet resistance even after the first bending. In the case of the monolayer graphene with/without the chlorine doping, the sheet resistance was initially increased possibly due to defect formation on the graphene; however, after 1400 times bending, the resistance remained almost the same. In addition, the sheet resistances of the graphene were almost the same with/without chlorine doping. It indicates that the graphene doping through low energy chlorine adsorption did not change the mechanical properties of the monolayer graphene film. In the case of bi- and tri-layers of graphene, the sheet resistance increased slightly at initial bending, and after that, it remained almost the same even after 1400 times bending cycles. Therefore, this cyclic low energy chlorine trap-doping strategy can be highly applicable to graphene transparent conductive films on flexible substrates, which require robust mechanical properties and reliability during bending, as well as high transparency and low sheet resistance.

Conclusion

In summary, a new doping method (cyclic trap-doping through low energy chlorine adsorption) was introduced to obtain a graphene film having the properties of low sheet resistance, high transparency, low damage and high thermal stability. After the low energy chlorine doping, the Raman results showed that the G and 2D peaks blue-shifted with no increase of the D peak, indicating doping without significant damage to the graphene. DF-TEM showed that chlorine atoms were trapped between the graphene layers by forming a network. After the cyclic chlorine trap-doping, we obtained a tri-layer

graphene-based PET film with a sheet resistance of 70 Ω per sq. at a transmittance of 94% at 550 nm. This means that this trap-doping through low energy chlorine adsorption can be an effective and controllable way to engineer the physical and electronic properties of graphene. The observed results on the sheet resistance and transmittance were improved beyond other previous results. Especially, if the thermal stability is considered additionally, this doping method could be a powerful technique. The graphene film doped by cyclic chlorine trap-doping also showed excellent flexibility and stability in the bending test. The cyclic chlorine trap-doping strategy introduced in this study can be applied to graphene used in various electronic applications such as printed electronics, flexible touch screens, transistors, integrated circuits, *etc.*

Experimental section

Synthesis of the graphene layer

Monolayer graphene films were synthesized on Cu foil by the chemical vapor deposition (CVD) method. Cu foil of 100 × 90 cm^2 area and 75 μm thickness was placed in a vacuum CVD quartz chamber. The temperature was increased up to 1050 °C in H_2, 10 sccm, and the foil was annealed for 1 h at this temperature prior to growth. Graphene was synthesized at 1050 °C by gas flow of H_2/CH_4, 10/20 sccm, for 30 min, and then the chamber was cooled down to room temperature with H_2 gas, 10 sccm, in 1 h. After the synthesis, the Cu foil was cut into small equal pieces (3 × 3 cm^2), coated with poly(methyl methacrylate) (PMMA), and immersed in a Cu etchant ($FeCl_3$) solution to etch away the Cu foil. When Cu was completely etched away, the graphene sheets with PMMA were rinsed in deionized water several times to wash away etchant residues. Then, PMMA-coated graphene sheets were transferred onto polyethylene terephthalate (PET), quartz and SiO_2 substrates. PMMA was removed with acetone for 30 min after the graphene had completely adhered to the substrates.

Cyclic trap-doping by low energy chlorine absorption and annealing (heating) procedure

The chlorine doping steps were repeated on the same graphene-coated substrate in order to maintain the cyclic chlorine trap-doping of the graphene sheets up to tri-layers. One cycle of trap-doping includes low energy chlorine doping on the top of the graphene, trapping of chlorine by the transfer of an additional graphene layer, and annealing at 250 °C for the SiO_2 and quartz substrates, and at 230 °C for the PET film for 30 min–6.5 h. The low energy chlorine doping was conducted with the inductively coupled plasma (ICP) system with a double-mesh grid shown in Fig. S1† using 10 mTorr 60 sccm Cl_2 at 20–300 W 13.56 MHz rf power. To minimize the adsorbed Cl dopant removal on the doped graphene surface during the transfer of the second or third graphene layers on the substrates with the doped graphene, the substrate with doped graphene was not dipped in the deionized (DI) water directly during the graphene transfer. Instead, the graphene was transferred on PET film first and the graphene on the PET film was transferred to the substrate with doped graphene. However, as shown in Fig. S6,† the fabricated doped graphene turned out to be extremely stable even for air exposure for more than 120 days, followed by DI water dipping for 3 hours, and followed by acetone cleaning for two hours. For the investigation of the thermal stability, the prepared graphene films were also heated at around 230–250 °C for 100 h in a vacuum furnace.

Characterization

Sheet resistance was measured using a sheet resistance meter (Dasoleng, FPP-2400) at room temperature for the graphene films on SiO_2 and PET. Ultraviolet-visible-near infrared (UV-Vis-NIR) absorption spectroscopy (Shimadzu, 3600) and Raman spectroscopy (Renishaw, RM-1000 Invia) with an excitation energy of 2.41 eV (514 nm, Ar^+ ion laser) were used to characterize the optical properties of the graphene films on the PET, quartz and SiO_2 substrates, respectively. For the observation of chlorine atom locations between the graphene layers prepared with/without the chlorine trapped doping, DF-TEM was used, and micro-EDS (energy dispersive X-ray spectroscopy) installed in the TEM was used for the analysis of components in Cl trapped area for a chlorine trap doped bilayer graphene. The graphene surface was investigated using angle resolved X-ray photoelectron spectroscopy (ARXPS, ESCA2000, VG Microtech Inc.) using an Mg Kα twin-anode source. To observe the carbon binding states near the surface, the take-off angle was fixed at 45°. The bending test of the graphene coated on PET was carried out under the bending conditions of a curvature radius of 5.0 mm and a bending frequency of 1 Hz using an in-house bending test machine.

Acknowledgements

This research was supported by Nano Material Technology Development Program through the National Research Foundation of Korea (NRF) funded by the Ministry of Education, Science and Technology (2012M3A7B4035323), and was also supported by the MOTIE (Ministry of Trade, Industry & Energy) (10048504) and KSRC (Korea Semiconductor Research Consortium) support program for the development of the future semiconductor device.

Notes and references

1 K. S. Novoselov, A. K. Geim, S. V. Morozov, Y. Zhang, S. V. Dubonos, I. V. Grigorieva and A. A. Firsov, *Science*, 2004, **306**, 666–669.
2 K. S. Novoselov, A. K. Geim, S. V. Morozov, D. Jiang, M. I. Katsnelson, I. V. Grigorieva, S. V. Dubonos and A. A. Firsov, *Nature*, 2005, **438**, 197–200.
3 C. R. Dean, A. F. Young, C. Lee, L. Wang, S. Sorgenfrei, K. Watanabe, T. Taniguchi, P. Kim, K. L. Shepard and J. Hone, *Nat. Nanotechnol.*, 2010, **5**, 722–726.

4 F. Wang, Y. B. Zhang, C. Tian, C. Girit, A. Zettl, M. Crommie and Y. R. Shen, *Science*, 2008, **320**, 206–209.
5 N. O. Weiss, H. L. Zhou, L. Liao, Y. Liu, S. Jiang, Y. Huang and X. F. Duan, *Adv. Mater.*, 2012, **24**, 5782–5825.
6 A. K. Geim, *Science*, 2009, **324**, 1530–1534.
7 A. K. Geim and K. S. Novoselov, *Nat. Mater.*, 2007, **6**, 183–191.
8 S. K. Bae, H. K. Kim, Y. B. Lee, X. F. Yu, J. S. Park, Y. Zheng, J. Balakrishnan, T. Lei, H. R. Kim, Y. I. Song, Y. J. Kim, K. S. Kim, B. Ozyilmaz, J. H. Ahn, B. H. Hong and S. Iijima, *Nat. Nanotechnol.*, 2010, **5**, 574–578.
9 D. Langley, G. Giusti, C. Mayousse, C. Celle, D. Bellet and J. P. Simonato, *Nanotechnology*, 2013, **24**, 452001.
10 C. Mattevi, H. W. Kim and M. Chhowalla, *J. Mater. Chem.*, 2011, **21**, 3324–3334.
11 F. Gunes, H. J. Shin, C. Biswas, G. H. Han, E. S. Kim, S. J. Chae, J. Y. Choi and Y. H. Lee, *ACS Nano*, 2010, **4**, 4595–4600.
12 J. Zheng, H. T. Liu, B. Wu, C. A. Di, Y. L. Guo, T. Wu, G. Yu, Y. Q. Liu and D. B. Zhu, *Sci. Rep.*, 2012, **2**, 662.
13 U. N. Maiti, W. J. Lee, J. M. Lee, Y. T. Oh, J. Y. Kim, J. E. Kim, J. W. Shim, T. H. Han and S. O. Kim, *Adv. Mater.*, 2014, **26**, 40–67.
14 D. S. Hecht, L. B. Hu and G. Irvin, *Adv. Mater.*, 2011, **23**, 1482–1513.
15 X. Huang, C. L. Tan, Z. Yin and H. Zhang, *Adv. Mater.*, 2014, **26**, 2185–2204.
16 M. Wang, S. K. Jang, W. J. Jang, M. W. Kim, S. Y. Park, S. W. Kim, S. J. Kahng, J. Y. Choi, R. S. Rouff, Y. J. Song and S. J. Lee, *Adv. Mater.*, 2013, **25**, 2746–2752.
17 H. Liu, Y. Liu and D. Zhu, *J. Mater. Chem.*, 2011, **21**, 3335–3345.
18 X. Zhang, A. Hsu, H. Wang, Y. Song, J. Kong, M. S. Dresselhaus and T. Palacios, *ACS Nano*, 2013, **7**, 7262–7270.
19 J. Wu, L. Xie, Y. G. Li, H. L. Wang, Y. Ouyang, J. Guo and H. Dai, *J. Am. Chem. Soc.*, 2011, **13**, 19668–19671.
20 Q. Zheng, Z. Li, J. Yang and J. K. Kim, *Prog. Mater. Sci.*, 2014, **64**, 200–247.
21 Y. Wang, C. Di, Y. Liu, H. Kajiura, S. Ye, L. Cao, D. Wei, H. Zhang, Y. Li and K. Noda, *Adv. Mater.*, 2008, **20**, 4442–4449.
22 Q. B. Zheng, M. M. Gudarzi, S. J. Wang, Y. Geng, Z. Li and J.-K. Kim, *Carbon*, 2011, **49**, 2905–2916.
23 P. Barpanda, G. Fanchini and G. G. Amatucci, *Carbon*, 2011, **49**, 2538–2548.
24 Q. Zheng, W. H. Ip, X. Lin, N. Yousefi, K. K. Yeung, Z. Li and J. K. Kim, *ACS Nano*, 2011, **7**, 6039–6051.
25 B. Li, L. Zhou, D. Wu, H. Peng, K. Yan and Z. F. Liu, *ACS Nano*, 2011, **5**, 5957–5961.
26 Y. C. Lin, C. C. Lu, C. H. Yeh, C. H. Jin, K. Suenaga and P. W. Chiu, *Nano Lett.*, 2012, **12**, 414–419.
27 M. W. Iqbal, A. K. Singh, M. Z. Iqbal and J. H. Eom, *J. Phys.: Condens. Matter*, 2012, **24**, 335301.
28 Z. Ni, Y. Wang and Z. Shen, *Nano Res.*, 2008, **1**, 273–291.
29 Y. Zhu, D. K. James and J. M. Tour, *Adv. Mater.*, 2012, **24**, 4924–4955.
30 S. Tongay, K. Berke, M. Lemaitre, Z. Nasrollahi, D. B. Tanner, A. F. Hebard and B. R. Appleton, *Nanotechnology*, 2011, **22**, 425701.
31 K. K. Kim, A. Reina, Y. Shi, H. Park, L. J. Li, Y. H. Lee and J. Kong, *Nanotechnology*, 2010, **21**, 285205.

